

ORIGINAL ARTICLE

# The Effect of Fractal Contact Lenses on Peripheral Refraction in Myopic Model Eyes

Manuel Rodriguez-Vallejo<sup>1,2</sup>, Josefa Benlloch<sup>2</sup>, Amparo Pons<sup>2</sup>,  
Juan A. Monsoriu<sup>1</sup> and Walter D. Furlan<sup>2</sup>

<sup>1</sup>Centro de Tecnologías Físicas, Universitat Politècnica de València, Valencia, Spain and

<sup>2</sup>Departamento de Óptica, Universitat de València, Burjassot, Spain

## ABSTRACT

**Purpose:** To test multizone contact lenses in model eyes: Fractal Contact Lenses (FCLs), designed to induce myopic peripheral refractive error (PRE).

**Methods:** Zemax ray-tracing software was employed to simulate myopic and accommodation-dependent model eyes fitted with FCLs. PRE, defined in terms of mean sphere  $M$  and  $90^\circ$ – $180^\circ$  astigmatism  $J_{180}$ , was computed at different peripheral positions, ranging from  $0$  to  $35^\circ$  in steps of  $5^\circ$ , and for different pupil diameters (PDs). Simulated visual performance and changes in the PRE were also analyzed for contact lens decentration and model eye accommodation. For comparison purposes, the same simulations were performed with another commercially available contact lens designed for the same intended use: the Dual Focus (DF).

**Results:** PRE was greater with FCL than with DF when both designs were tested for a 3.5 mm PD, and with and without decentration of the lenses. However, PRE depended on PD with both multizone lenses, with a remarkable reduction of the myopic relative effect for a PD of 5.5 mm. The myopic PRE with contact lenses decreased as the myopic refractive error increased, but this could be compensated by increasing the power of treatment zones. A peripheral myopic shift was also induced by the FCLs in the accommodated model eye. In regard to visual performance, a myopia under-correction with reference to the circle of least confusion was obtained in all cases for a 5.5 mm PD. The ghost images, generated by treatment zones of FCL, were dimmer than the ones produced with DF lens of the same power.

**Conclusions:** FCLs produce a peripheral myopic defocus without compromising central vision in photopic conditions. FCLs have several design parameters that can be varied to obtain optimum results: lens diameter, number of zones, addition and asphericity; resulting in a very promising customized lens for the treatment of myopia progression.

**Keywords:** Contact lenses, model eyes, myopia, myopia progression, peripheral refraction

## INTRODUCTION

The treatment of myopia progression deserves the attention of ophthalmologists and optometrists mainly because of the high risk of serious ophthalmic diseases associated with it.<sup>1,2</sup> Experimental studies in animals<sup>3,4</sup> found that refractive error in the peripheral retina can regulate the eye growth, in particular, relative peripheral hyperopia has been suggested as

a possible factor that could cause the progression of myopia (see Smith<sup>4</sup> for a review). Consequently, the induction of a myopic peripheral refractive error (PRE) could be considered as a myopia progression treatment in humans, taking into consideration that retina<sup>5</sup> is able to identify positive and negative defocus, and paracentral retina reacts more vigorously than central retina to optical defocus.<sup>6</sup> This finding may be related to sign-dependent sensitivity to

peripheral defocus for myopes,<sup>7</sup> which could be due to specific combinations of eye aberrations at peripheral retina.<sup>8-10</sup>

Based on this theory, different optical treatment strategies have been proposed and tested.<sup>11-13</sup> With regard to soft contact lenses, the effect on peripheral refraction<sup>14,15</sup> and on myopia progression<sup>16</sup> of several designs for presbyopia have also been investigated, but these lenses showed a negative impact on foveal vision because of the nature of their designs.<sup>17</sup> Consequently, new contact lenses have been proposed specifically for myopia treatment.<sup>18,19</sup> Unfortunately, little information is available concerning the impact on peripheral refraction of different variables such as pupil diameter (PD), refractive error, lens decentration and therapeutic power. In this sense, we think that some improvements could be obtained by making ray-tracing simulations on model eyes with a careful optimization of several lens design parameters.

Different human model eyes can be used to perform such simulations. For instance, the *Model 1* proposed by Atchison,<sup>20</sup> derived from experimental data, reflects the refraction related changes of the eye. It has been demonstrated that this model gives good predictions of the hyperopic peripheral shift in the mean sphere along the nasal visual field in myopic eyes,<sup>21,22</sup> and it has also been employed to study the effect on PRE of contact lenses with different degrees of asphericity.<sup>20</sup> Nevertheless, this model does not predict changes in the eye power with accommodation. The accommodation-dependent model eye proposed by Navarro & Santamaria<sup>23</sup> represents an alternative to Atchison's model to simulate the relative effect of the accommodation on the PRE of an emmetropic eye.

In this work, a new contact lens design is presented as a potential therapeutic method for the treatment of myopia progression. These lenses have been specifically designed to correct the foveal refractive error of the eye and simultaneously to generate a myopic refractive error along the peripheral retina. Our design, named Fractal Contact Lens (FCL),<sup>24</sup> is inspired on Fractal Zone Plates, which are multifocal diffractive lenses characterized by a fractal focal structure (i.e. self-replicating pattern at different scales) along the optical axis.<sup>25</sup> Under white-light illumination, this property optimizes their performance as image forming devices, because it makes them with an extended depth of field and a reduced chromatic aberration.<sup>26</sup> Different ophthalmic optical elements in the form of multifocal intraocular lenses and multifocal contact lenses have been proposed based on Fractal zone plates.<sup>24</sup> In particular, the FCLs for myopia treatment<sup>27</sup> are multi-zone contact lenses with a larger central zone than those intended for presbyopia correction, previously developed.<sup>24</sup> The outer zones of the FCLs are designed to obtain a myopic PRE without producing a secondary image

at the central fovea in normal photopic vision and to not interfere with the normal functioning of the accommodation system in myopic young subjects. Simulations of the FCLs performance in model eyes are simulated with Zemax ray tracing software and compared with those calculated by the use of another contact lens specifically proposed for the treatment of myopia progression: The Dual Focus (DF).<sup>19</sup> Our purpose is to show that FCLs can improve the optical performance of the DF lenses, producing a higher myopic PRE without compromising the foveal image quality over a wide range of viewing conditions.

## METHODS

### Contact Lenses

FCL design for myopia treatment consists of six refractive zones, (three correction (C) zones and three treatment (T) zones). The radii of the zones are distributed from center to periphery according to the triadic fractal Cantor set<sup>25,28</sup> along of the squared radial coordinate. As illustrated in Figure 1(A), the diameters of the FCL zones are  $C_1=4.50$  mm,  $T_1=6.50$  mm,  $C_2=7.91$  mm,  $T_2=11.42$  mm,  $C_3=12.27$  mm and  $T_3=13.14$  mm. The optical power of the correction zones compensates the refractive error of the eye, while the treatment zones produce simultaneously a myopic focus on the peripheral retina without affecting the foveal image, at least under photopic conditions. In this way, a FCL behaves as a multi-zone refractive lens, with negligible diffractive effects because it has a relatively low number of wide zones.<sup>27</sup> The other lens chosen for comparison (Figure 1B): The DF soft contact lens<sup>19,29</sup> has three correction (C) and two treatment (T) zones. From center to periphery, the diameter of the zones are

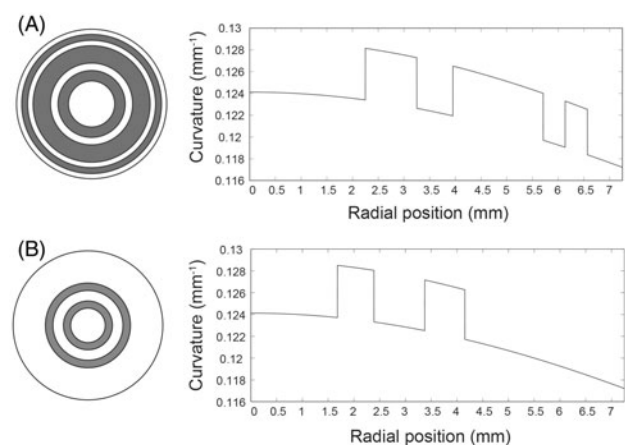


FIGURE 1 Graphical sketch of (A) FCL and (B) DF lens. Front view with zone sizes in gray for treatment zones and white for correction zones (left), and a section view with the curvature along the radial position (right).

$C_1 = 3.36$  mm,  $T_1 = 4.78$  mm,  $C_2 = 6.75$  mm,  $T_2 = 8.31$  mm and  $C_3 = 11.66$  mm (Figure 1B).

**Ray-Tracing**

The performance of our designs was tested by ray-tracing simulations using a commercially available software package (Zemax 13 SE; Zemax Development Corporation, Bellevue, WA). Myopic eyes were simulated with the model eye proposed and tested by Atchison<sup>20</sup> (*Model 1*) because this model includes spectacle refraction-related changes of the anterior corneal radius, vitreous length and retinal shape, and accurately predicts the hyperopic peripheral shift in the mean sphere measured in myopic eyes along the nasal visual field. However, this model eye does not allow different levels of accommodation. Therefore, instead of the myopic *Model 1*, the Navarro<sup>23</sup> model eye was employed to simulate accommodated eyes. Even though Navarro model does not contemplate different refractive errors, its use in this work is justified because it has been found that the effect of accommodation on PRE (mean sphere and astigmatism) is not significantly different between emmetropic and myopic eyes.<sup>30–32</sup> Tables 1 and 2 show the Zemax parameters taken from the spreadsheet program for the *Model 1* and Navarro models, respectively.

As the model eyes are rotationally symmetric, PREs were computed only across one horizontal semi-meridian of the eye in steps of 5°, from 0° to 35°. To determine the PREs, we followed a similar procedure as the one described in Ref. [20], i.e. for each angle of eccentricity, a thin lens (a *paraxialXY*<sup>33</sup> surface in Zemax) was located 0.2 mm in front of the cornea with a different value of tilt and decentration depending on the angle subtended by

TABLE 1 Atchison myopic model eye parameters with spectacle refraction (SR) in D.

| Zemax $n^\circ$ : type   | Refractive index (Medium) (555 nm) | Radius (mm) | Thickness (mm) | Asphericity |
|--------------------------|------------------------------------|-------------|----------------|-------------|
| 1: Standard              | 1 (air)                            |             |                |             |
| 2: Standard              | 1.376 (cornea ant.)                | rc          | 0.55           | -0.15       |
| 3: Standard              | 1.3374 (cornea post.)              | 6.4         | 3.15           | -0.275      |
| 4: Standard <sup>a</sup> | 1.3374 (pupil)                     | Inf.        | 0              | 0           |
| 5: Gradient              | Grad A (ant. lens)                 | 11.48       | 1.44           | -5          |
| 6: Gradient              | Grad P (equator)                   | Inf.        | 2.16           | 0           |
| 7: Standard              | 1.336 (post. lens)                 | -5.90       | v1             | -2          |
| 8: Biconic               | (retina)                           | rx, ry      |                | Qx, Qy      |

rc = 7.77 + 0.022SR.  
 Grad A = 1.371 + 0.0652778Z - 0.0226659 Z<sup>2</sup> - 0.0020399(X<sup>2</sup> + Y<sup>2</sup>).  
 Grad P = 1.418 - 0.0100737 Z<sup>2</sup> - 0.0020399(X<sup>2</sup> + Y<sup>2</sup>).  
 v1 = 16.28 - 0.299SR.  
 rx = -12.91 - 0.094SR Qx = 0.27 + 0.026SR.  
 ry = -12.72 + 0.0045SR Qy = 0.25 + 0.017SR.  
<sup>a</sup>Aperture type: float by stop size.

the chief ray. The *paraxialXY* surface acts as an ideal thin lens with optical power specified in two directions, ( $F_x$ ) and ( $F_y$ ).<sup>33</sup> Zemax Programming Language was employed to perform an optimization routine in attempt to obtain, for each angle, the values of  $F_x$  and  $F_y$  that minimize the RMS spot radius with respect to the centroid. Decentrations and tilts were made by the Zemax *coordinate break surface* capability, applying decentrations before tilts and reversing the *coordinate break surface* before ray-tracing to the cornea. Table 3 shows the decentration and tilt values applied to *paraxialXY* surface and the respective position where the chief ray intersects the cornea. With the values of the parameters  $F_x$  and  $F_y$  given by the routine, the mean sphere  $M$  and the 90°–180° astigmatism  $J_{180}$  were obtained from:<sup>20</sup>

$$M = (F_x + F_y)/2$$

$$J_{180} = (F_x - F_y)/2 \tag{1}$$

The same Zemax procedure was performed with FCL and DF. The contact lenses were located between the *paraxialXY* surface and the cornea. The front surface of the contact lenses was modeled using a ZEMAX *Binary Optic 4* surface, which supports a

TABLE 2 Escudero-Navarro model eye parameters with accommodation A in D.

| Zemax $n^\circ$ : type   | Refractive index (Medium) (555 nm) | Radius (mm)    | Thickness (mm) | Asphericity    |
|--------------------------|------------------------------------|----------------|----------------|----------------|
| 1: Standard              | 1 (air)                            |                |                |                |
| 2: Standard              | 1.376 (cornea ant.)                | 7.72           | 0.55           | -0.26          |
| 3: Standard              | 1.3374 (cornea post.)              | 6.5            | d <sub>2</sub> | 0              |
| 4: Standard <sup>a</sup> | 1.3374 (Pupil)                     | Inf.           | 0              | 0              |
| 5: Gradient              | n3 (ant. lens)                     | R <sub>3</sub> | d <sub>3</sub> | Q <sub>3</sub> |
| 6: Standard              | 1.336 (post. lens)                 | R <sub>4</sub> | 16.40398       | Q <sub>3</sub> |
| 7: Biconic               | (Retina)                           | -12            |                | Q <sub>4</sub> |

R<sub>3</sub> = 10.2 - 1.75 ln (A + 1).  
 R<sub>4</sub> = -6.0 + 0.2294 ln (A + 1).  
 d<sub>2</sub> = 3.05 - 0.05 ln (A + 1).  
 d<sub>3</sub> = 4.00 + 0.1 ln (A + 1).  
 n<sub>3</sub> = 1.42 + 9 × 10<sup>-5</sup> (10A + A<sup>2</sup>).  
 Q<sub>3</sub> = -3.1316 - 0.34 ln (A + 1).  
 Q<sub>4</sub> = -1.0 - 0.125 ln (A + 1).  
<sup>a</sup>Aperture type: float by stop size.

TABLE 3 Decenter/tilt values applied to the *paraxialXY* surface for each measure along the visual field.

| Visual field | Dec.X (mm) | Tilt-Y (°) |
|--------------|------------|------------|
| 40           | 3          | -40        |
| 35           | 2.3        | -35        |
| 30           | 1.95       | -30        |
| 25           | 1.6        | -25        |
| 20           | 1.25       | -20        |
| 15           | 0.9        | -15        |
| 10           | 0.6        | -10        |
| 5            | 0.3        | -5         |

variable number of concentric radial zones of different powers with independent: radial size, conic and polynomial aspheric deformation. Although it has not been used in our simulations, all zones may also have a diffractive phase profile with independent coefficients.<sup>33</sup>

Despite the fact that FCLs can be fabricated in both soft and rigid gas permeable materials, in this work, we restricted the analysis to soft contact lenses in order to obtain results that could be compared with those obtained with DF. Considering soft contact lens flexure, the back surface radii ( $r_b$ ) of contact lenses were considered the same of the cornea. The front radii ( $r$ ) of the zones were calculated in terms of the back vertex power (BVP) as:

$$r = \frac{r_b(n_l - 1)}{n_l - 1 + (r_b \text{ BVP})} - \frac{t_c}{n_l} + t_c \quad (2)$$

where  $t_c = 0.1$  mm is the thickness at the center of the contact lenses and  $n_l = 1.403$  is the refractive index for the wavelength of 555 nm. We assumed that the asphericity of the contact lens surfaces matched the corresponding values of the model cornea (see Tables 1 and 2) since, as we mentioned above, soft contact lenses conform exactly to the front corneal surface. This fact has been demonstrated in experimental studies,<sup>34–36</sup> and justified in previous theoretical calculations.<sup>37</sup> It is also important to note that model eyes do not consider changes to the curvature beyond the cornea (scleral curvature), therefore if back surface of the contact lens is considered with the same asphericity of the cornea, a perfect alignment will be obtained when  $r_b$  is similar to the cornea radius. The refractive index at the back surface of the contact lenses was set  $n = 1$  (air) and a thin tear film ( $n = 1.336$ ) was placed between the cornea and the contact lenses with the same curvature as both surfaces.

With the Zernike coefficients provided by Zemax, foveal images were simulated numerically using the standard Fourier techniques following the procedure detailed in Ref. Legras *et al.*<sup>38</sup>, i.e. by computing the optical transfer function (OTF) of the model eye wearing each type of lenses under different conditions. The image of the object was finally obtained by multiplying the computed OTF with the Fourier spectrum of the object (a set of optotypes) and doing an inverse Fourier transform.

Finally, PRE was computed with and without FCL using the accommodated and unaccommodated Navarro model eye. We decided to use a PD of 3.5 mm for this analysis considering that near work is normally performed under photopic illumination. The same procedure that described previously with the myopic model was performed with two little variations. First, the soft contact lens parameters were fitted in accordance to the cornea parameters

of the Navarro model. Second, the object was placed at infinity for distance vision and at 33.3 cm in front the cornea (3.00 D for near vision).

## RESULTS

The FLC performance was first evaluated for a treatment zone power (TP) of +2.00 D in order to obtain results that could be compared with those obtained with the DF lens, which has been designed with the same TP. Figure 2 shows the PRE computed for myopic eyes along the horizontal meridian, up to 35° of visual field angle. Results for two myopic eyes are represented in Figure 2: –2.00 D (panels A and B), and –8.00 D (panels C and D) for two PDs, 3.5 mm and 5.5 mm. These correspond approximately to PDs of a 10-year-old child under photopic and mesopic levels of illumination, respectively.<sup>39</sup> Regarding the mean sphere  $M$ , two common features of both lenses can be observed in Figure 2(A) and in Figure 2(C): On the one hand, the relative peripheral myopic shift was lower for –8.00 D than for –2.00 D. We found that other values of myopia ranging between –2.00 D and –8.00 D (not shown) produced intermediate results. On the other hand, a central under-correction was obtained in all cases, except for the FCL with a PD of 3.5 mm. As can be seen, the amount of this under-correction was also dependent on the degree of myopia. This effect could be explained by the spherical aberration of the eye and by the relative influence of the treatment zones on central vision as PD increases. Note that, in spite of the fact that the PRE produced by both lenses was dependent on PD, the increase rate of the myopic shift with the eccentricity for a PD of 3.5 mm (circles in Figure 2) was greater with the FCL than with the DF lens.

Figures 2(B and D) illustrate the results obtained for 90°–180° astigmatism  $J_{180}$ . As happened with mean sphere, the peripheral astigmatism produced by both lenses was dependent on the PD but to a lower degree than  $M$ . Note that the peripheral astigmatism at 35° was higher for FCL than for DF.

Figure 3 shows the effect of lens misalignment on PRE mean sphere. The values obtained for a FCL (Figure 3A) and DF (Figure 3B) centered on the eye's pupil were compared with those obtained when the lenses were decentered 0.5 mm downward and 0.5 mm to the temporal side. It can be seen that for a PD of 3.5 mm (circles), the influence of decentration was of less importance for FCL than for DF. In fact, higher values of PRE were obtained with FCL design. Related to the previous result, Figure 4 shows the foveal images computed numerically. As can be seen, although both lenses have similar performance for a PD of 5.5 mm, the ghost images produced by the near focus are clearly more evident in the images



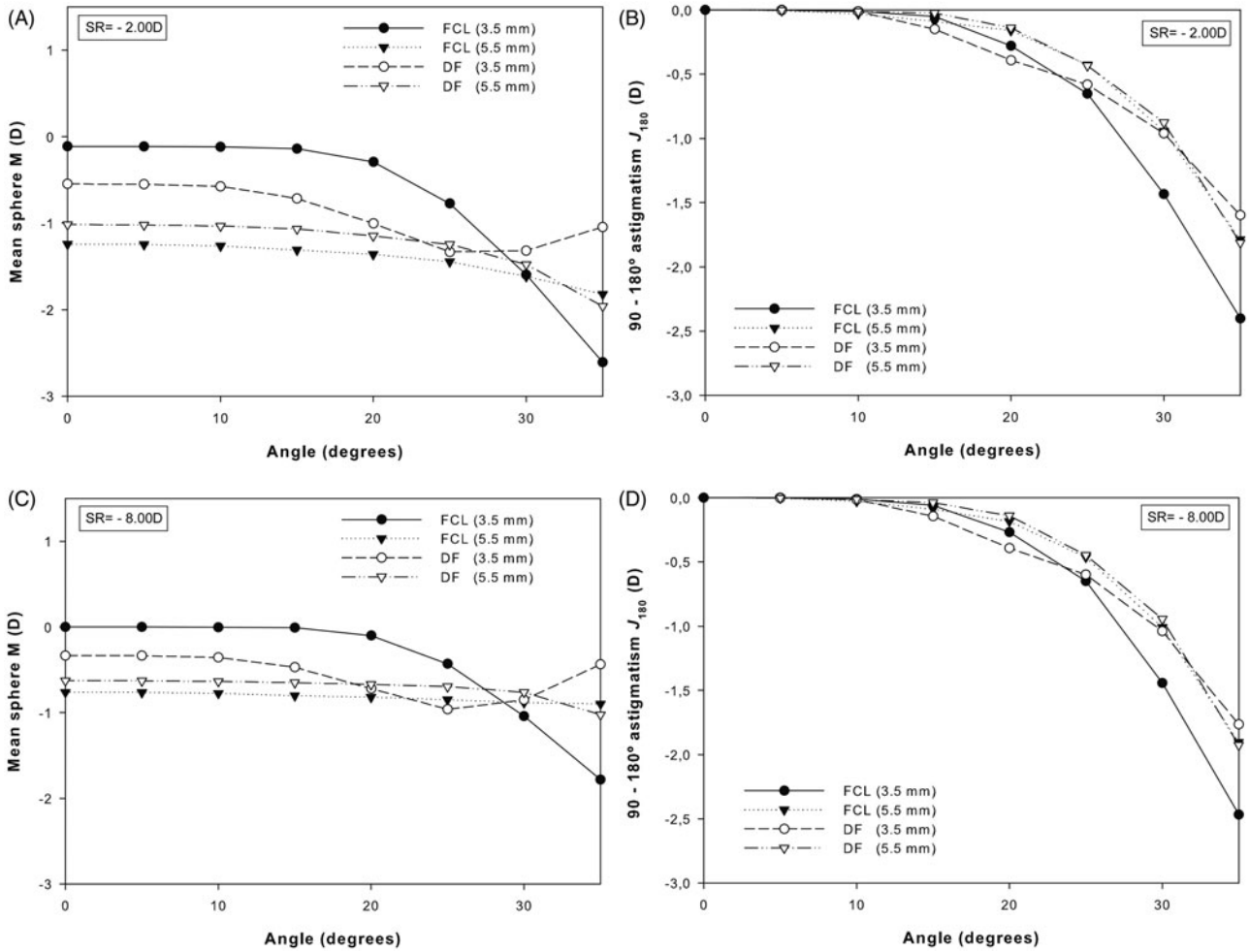


FIGURE 2 Mean sphere  $M$  (left) and astigmatism  $J_{180}$  (right) as a function of the visual field for  $-2.00$  D (top) and  $-8.00$  D (bottom) in the myopic Atchison model eye compensated with FCLs and DF lenses for pupil diameters of 3.5 and 5.5 mm.

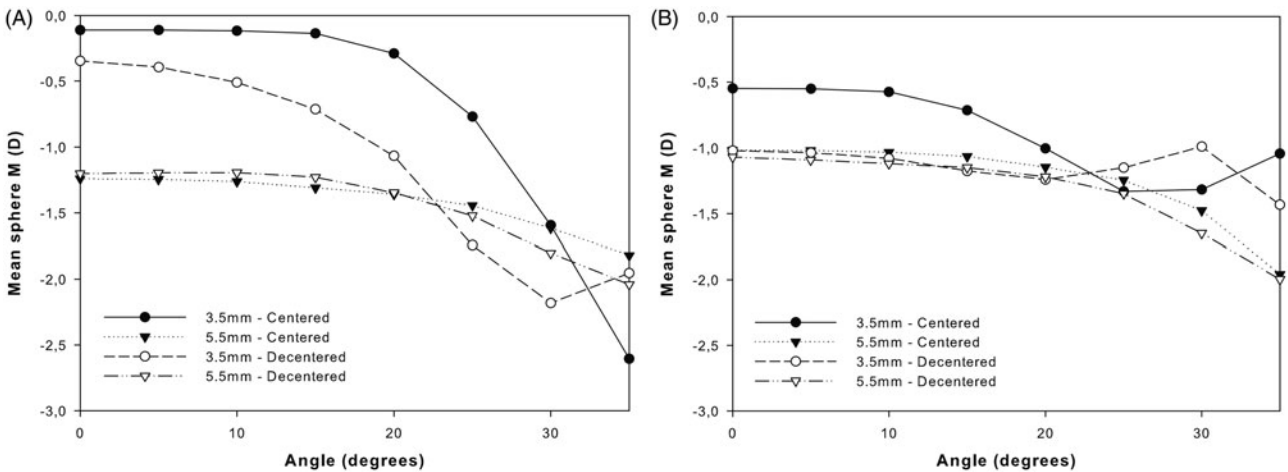


FIGURE 3 Impact of lens decentration on mean sphere ( $M$ ) as a function of the visual field for a myopic model eye of  $-2.00$  D compensated with FCL (left) and DF (right). Closed symbols correspond to a centered lens. Open symbols correspond to a lens decentered 0.5 mm downward and 0.5 mm to the temporal side.

corresponding to the DF lens. As we mentioned, FCL design admits different powers of treatment zone. The influence of this parameter on the PRE is represented in Figure 5 for a  $-2.00$  D myopic eye with a 3.5 mm

PD. As can be observed, the effect of TP variation was more noticeable for the mean sphere, than for  $90^{\circ}$ – $180^{\circ}$  astigmatism. As TP increased, the PRE also increased in all cases, with a maximum increase

for  $M$  at  $35^\circ$  of around 75% of the TP added, and nearly one half of this added value at  $30^\circ$ .

The performance of the FCL in near vision was simulated with the Navarro model eye for a PD of 3.5 mm. The results are shown in Figure 6. As can be

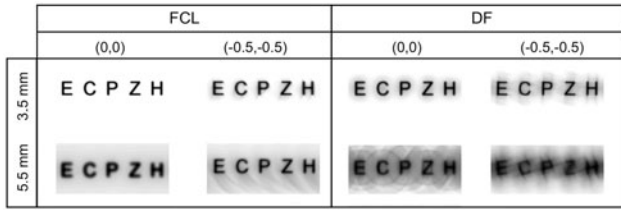


FIGURE 4 Simulated optical images at fovea of a  $-2.00$  D myopic model eye compensated with FCL (left) and DF (right). A 20/50 set of letters was used as object. Values in brackets represent a centered lens (0.0) and a decentered lens relative to the pupil ( $-0.5$  mm downward,  $-0.5$  mm temporal). Images correspond to two pupil diameters, 3.5 and 5.5 mm.

seen, when the accommodation was relaxed, the model eye without contact lens correction (naked eye [NE] curves in the figure) predicted that mean sphere PRE becomes more hyperopic as the peripheral angle increased. Then, a myopic shift was produced in the PRE in all cases for the accommodated eye (open symbols in the figure). Note that FCL produced a relative myopic shift, which reached its highest value at  $35^\circ$  for  $M$  and  $J_{180}$  in both cases, with accommodated and unaccommodated eye.

## DISCUSSION

### Peripheral Refractive Error

We found that the PRE obtained with FCL was higher than the one produced by DF for refractive errors in the range of  $-2.00$  D to  $-8.00$  D. However, our

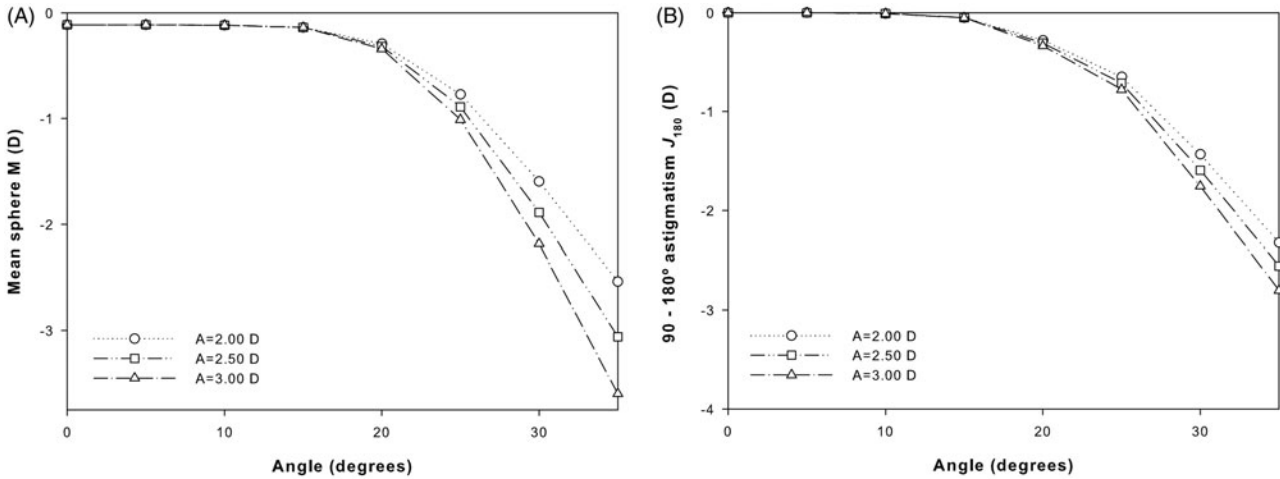


FIGURE 5 Mean sphere  $M$  (left) and astigmatism  $J_{180}$  (right) as a function of the visual field for a myopic model eye of  $-2.00$  D compensated with FCLs having different amount of treatment power (TP).

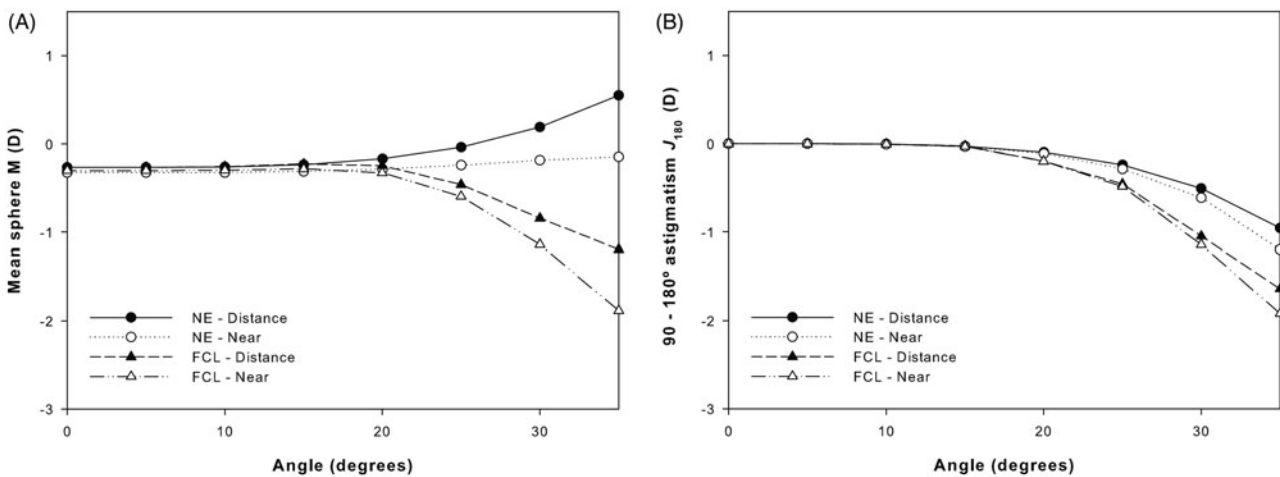


FIGURE 6 Mean sphere  $M$  (left) and astigmatism  $J_{180}$  (right) as a function of the visual field for an emmetropic unaccommodated (distance) and accommodated  $3.00$  D (near) Navarro model eye. Results for naked eye (NE), and fitted with a FCL with zero power at the correction zone and a therapeutic power of  $+2.00$  D.

results seem to suggest that the effectiveness of both types of lenses with a fixed treatment power might depend on the degree of myopia, since a lesser effect was obtained for higher values of myopia. These results are explained by the increase of the hyperopic PRE with the refractive error<sup>22</sup> that was properly modeled by Atchison.<sup>20</sup> Therefore, as the model eye is more hyperopic in the periphery with the increase of the refractive error, the total peripheral myopic shift obtained with the contact lens was lower. In our case, we have demonstrated that this limitation could be partially solved by increasing the value of the treatment power, since this is a free parameter in FCL design that affects the PRE without compromise central vision, at least for PDs lower than 4.0 mm.

Even though the impact on PRE produced by decentration of DF has not been previously reported, Sankaridurg et al.<sup>18</sup> found asymmetries in the PRE with another therapeutic contact lens designed to reduce relative peripheral hyperopia. The authors attributed this to the fact that contact lenses were decentered from the visual axis, centering, as contact lenses actually do, on the geometric center of the cornea. In our case, we also simulated the typical decentration of the lenses. As a result, we found that the PRE and the optical quality at the fovea were less sensitive to decentrations with FCL than with DF.

We also found that PD had a great impact in  $M$  at the periphery for both contact lens designs; therefore, we consider that therapeutic contact lenses should be designed to work optimally under photopic conditions. As far as the position of the first treatment zone is concerned, Anstice & Phillips<sup>19</sup> measured PDs in eyes wearing DF in three different lighting conditions. They suggested as an advantage of their design that the inner treatment zone fall inside the limits of the pupil even if miosis by accommodation is induced. Our simulations seem to contradict this assumption because we found a higher myopic shift with FCL, in which the inner zone fall outside the pupil under photopic conditions. Our results have a good agreement with those obtained with the orthokeratology technique (OK), on which the optic zone diameter of the OK lenses performs a change in the cornea curvature generally outside the pupil at photopic conditions.<sup>40</sup>

With respect to the influence of the number and extension of zones, our design has more zones than DF in order to obtain a larger therapeutic area affecting peripheral vision, since it has been hypothesized that effectiveness in myopia progression might be dependent on the extension of visual field that is manipulated.<sup>41</sup> In fact, Sankaridurg et al.<sup>42</sup> compared myopia progression with different designs of spectacle lenses. They found that the slowest progression resulted with the spectacle lenses with the most extended treatment area.

Regarding to the values obtained for peripheral astigmatism, which has also been suggested as a variable involved in myopia progression,<sup>43,44</sup> we found that FCL and DF lenses produced a similar effect: the values of  $J_{180}$  decreased with the eccentricity and, contrary to what happened for the mean sphere, it was nearly independent of the refractive error and less sensitive to the PD. Furthermore, our results (Figures 1, 5 and 6) allow to estimate the relative positions of the peripheral sagittal and tangential foci. In fact, from the variations of the mean sphere ( $M$ ) and the astigmatic component  $J_{180}$  with the eccentricity, two features can be deduced. First, at least under photopic conditions, FCL causes that the entirety of the interval of Sturm lies in front of the peripheral retina, while the central image is positioned at the fovea. Second, the sagittal focus is more sensitive to the eccentricity than the tangential focus, because it moves away from the retina faster as the angle of incidence increases. However, our results for the mean astigmatism  $J_{180}$  should be interpreted with caution and they need to be confirmed in the future with the outcome of clinical research, since the Atchison eye Model 1 overestimates this parameter by about 50%.<sup>20</sup>

## Visual Performance

As we have shown, visual performance could be influenced by multizone contact lenses. DF and FCL produced an under-correction for the myopia refractive error, which was dependent on the PD. As we mentioned, this effect could be attributed to the spherical aberration and the impact on foveal vision of the treatment zones with increasing PD. In fact, this under-correction was negligible with FCLs for PDs up to around 4 mm. Kollbaum et al.<sup>17</sup> pointed out that patients wearing DF lenses may experience some decrease in visual performance similar to that obtained with contact lenses for presbyopia; but in their work, it was not mentioned if lens centering and PD had been controlled. Although under-correction has been reported as a myopiogenic stimulus,<sup>45</sup> according to the very good clinical results reported with DF lenses<sup>19</sup> and other multifocal contact lenses,<sup>16</sup> it seems that this effect would be of little importance. Smith<sup>41</sup> explained this fact considering that foveal myopic defocus around 0.50–0.75 D does not create a myopic peripheral defocus under certain conditions. For instance, for fixation distances inside 1 m, it is likely that the foveal image will be in good focus and the eye will also experience peripheral hyperopia. However, in this situation, multifocal contact lenses also create a peripheral myopic defocus.<sup>46</sup> This may explain the positive results in slowing myopia progression with multifocal contact lenses in contrast to those

obtained with monofocal contact lenses producing an under-correction of the refractive error.

### Effect of the Accommodation

Although the Navarro model eye was not designed to predict the PRE, it has been used for the analysis of the relative change of the PRE due to the accommodation.<sup>47</sup> Our results predicted that the peripheral hyperopic defocus generated by the NE decreased as the accommodation increased. From an optical design stand point, the change in peripheral refraction could be attributed to an increase in the curvature of field and to an increase in the amount of peripheral astigmatism of the eye on accommodation.<sup>48</sup>

FCLs have been designed to not interfere with the normal functioning of accommodation; i.e. to avoid any additional blur at near vision under photopic lighting conditions. Therefore, the central zone of FCL covers the whole pupil area in this condition as opposed to DF on which the central zone is smaller.<sup>19</sup> According to our results, the FCL fitted to the Navarro<sup>23</sup> model eye produced a *beneficial* relative myopic shift, both with and without accommodation; i.e. the FCLs produced a relatively more myopic PRE at distance focus, which is maintained when the eye focused on a near object. Although we performed simulations with an emmetropic model eye, in our opinion these results might be extended to myopic eyes because, as we already mentioned, experimental evidence shows that the PRE profiles does not differ between emmetropes and myopes during accommodation.<sup>30–32</sup>

### Limitations of the Ray Tracing Simulations

Some limitations of this study are related to the model eyes employed. In spite of being the best option that we found for this purpose, these are far from being perfect models. In fact, as we mentioned above, Atchison Model 1 does not predict correctly the PRE along the vertical meridian and temporal visual field. Actually, clinical evidences of the PRE asymmetries in the visual field,<sup>20</sup> and the impact of accommodation on the PRE in myopes<sup>47</sup> are not fully predictable with any current model eye. In addition, we are aware of new accommodated model eyes that have been appeared,<sup>49</sup> but they were not considered in this study because they require special surfaces not supported by the Zemax SE version. Therefore, future improvements may be developed with the progress of the models and higher versions of Zemax.

In our simulations, we also assumed that soft contact lenses perfectly match the corneal surface.

Although this assumption could be questioned, images obtained recently with ultra-high resolution OCT do support it<sup>50</sup> and are in agreement with findings of earlier studies obtained with a high illumination keratometer<sup>34</sup> and a Shack–Hartmann aberrometer.<sup>51</sup> We have to recognize that we cannot directly extrapolate the results from our simulations to real efficacy of the lenses in clinic because of the above limitations. In addition, as like any other soft contact lens several variables will also influence the actual shape and performance of the contact lens on the eye: manufacturing technology,<sup>52</sup> lens materials,<sup>53</sup> tear film,<sup>54</sup> movement and flexure,<sup>55</sup> etc. With regard to DF lens, we want to point out that our simulated design could not correspond exactly with the commercial lenses, since we retrieved its shape from the literature and we have not characterized the real contact lens.

## CONCLUSIONS

In our opinion, ray tracing routines in model eyes can be considered as a versatile and fast procedure that could be very useful for predicting the outcomes of different lenses designed to slow the progression of myopia. Thus, the performance of a new design of soft contact lens for treatment of myopia progression (FCL) has been analyzed by ray tracing with Zemax 13 SE on the Atchison and Navarro model eyes. Results were compared with those provided by other soft contact lens designed for the same purpose (DF). According to our results, FCL performance was in general better than DF in terms of PRE and visual performance when contact lenses were evaluated under photopic conditions.

In spite of the previously discussed limitations, we believe that simulations performed in this work demonstrate the potentiality of the FCLs to produce a myopic relative peripheral error, which has been proposed as an optical treatment for myopia progression. In addition, we showed that the results are dependent on the PD; therefore changes in the design could be required depending on the patient. For this purpose, several design parameters can be adjusted in FCL to obtain the desired peripheral shift, such as diameter, number of zones, power of the treatment zone and asphericity. It is expected that clinical research will confirm our predictions about the PRE induced by FCLs. Finally, it is worth noting that FCL construction requires the same lathe technology employed in the fabrication of other commercial multizone contact lenses. Therefore, there are no special needs for its production. In fact, we are currently manufacturing the first prototypes of our designs intended to perform a long-term clinical study.



## ACKNOWLEDGEMENTS

The authors wish to thank Dr. Laura Remón for her help in obtaining the simulations of retinal images. Two anonymous reviewers are also acknowledged for their comments.

## DECLARATION OF INTEREST

The author(s) have made the following disclosure(s):

J. B.: None; M. R.-V., A. P., J. A. M. and W. D. F. inventors (P) ES Patent P201330862, relating to contact lens design: assigned to Universitat Politècnica de València and Universitat de València.

This research was supported by the Ministerio de Economía y Competitividad (grant FIS2011-23175), the Generalitat Valenciana (grant PROMETEO2009-077) and the Universitat Politècnica de València (grant INNOVA SP20120569), Spain.

## REFERENCES

- Gwiazda J. Treatment options for myopia. *Optom Vis Sci* 2009;86:624–628.
- Tarutta E, Chua W-H, Young T, Goldschmidt E, Saw SM, Rose KA, et al. Myopia: Why study the mechanisms of myopia? Novel approaches to risk factors signalling eye growth – how could basic biology be translated into clinical insights? Where are genetic and proteomic approaches leading? How does visual function contribute to and interact with ametropia? Does eye shape matter? Why ametropia at all? *Optom Vis Sci* 2011;88:404–447.
- Smith EL, Kee C, Ramamirtham R, Qiao-Grider Y, Hung L-F. Peripheral vision can influence eye growth and refractive development in infant monkeys. *Invest Ophthalmol Vis Sci* 2005;46:3965–3972.
- Smith EL. The Charles F. Prentice award lecture 2010: a case for peripheral optical treatment strategies for myopia. *Optom Vis Sci* 2012;88:1029–1044.
- Troilo D, Gottlieb MD, Wallman J. Visual deprivation causes myopia in chicks with optic nerve section. *Curr Eye Res* 1987;6:993–999.
- Ho W-C, Wong O-Y, Chan Y-C, Wong S-W, Kee C-S, Chan HH-L. Sign-dependent changes in retinal electrical activity with positive and negative defocus in the human eye. *Vis Res* 2012;52:47–53.
- Rosén R, Lundström L, Unsbo P. Sign-dependent sensitivity to peripheral defocus for myopes due to aberrations. *Invest Ophthalmol Vis Sci* 2012;53:7176–7182.
- Buehren T, Iskander DR, Collins MJ, Davis B. Potential higher-order aberration cues for spherocylindrical refractive error development. *Optom Vis Sci* 2007;84:163–174.
- Yamaguchi T, Ohnuma K, Konomi K, Satake Y, Shimazaki J, Negishi K. Peripheral optical quality and myopia progression in children. *Graefes Arch Clin Exp Ophthalmol* 2013;251:2451–2461.
- Thibos LN, Bradley A, Liu T, López-Gil N. Spherical aberration and the sign of defocus. *Optom Vis Sci* 2013;90:1284–1291.
- Tabernero J, Vazquez D, Seidemann A, Uttenweiler D, Schaeffel F. Effects of myopic spectacle correction and radial refractive gradient spectacles on peripheral refraction. *Vis Res* 2009;49:2176–2186.
- Ticak A, Walline JJ. Peripheral optics with bifocal soft and corneal reshaping contact lenses. *Optom Vis Sci* 2013;90:3–8.
- Santodomingo-Rubido J, Villa-Collar C, Gilmartin B, Gutiérrez-Ortega R. Myopia control with orthokeratology contact lenses in Spain: refractive and biometric changes. *Invest Ophthalmol Vis Sci* 2012;53:5060–5065.
- Rosén R, Jaeken B, Lindskoog Petterson A, Artal P, Unsbo P, Lundström L. Evaluating the peripheral optical effect of multifocal contact lenses. *Ophthalmic Physiol Opt* 2012;32:527–534.
- Kang P, Fan Y, Oh K, Trac K, Zhang F, Swarbrick HA. The effect of multifocal soft contact lenses on peripheral refraction. *Optom Vis Sci* 2013;90:658–666.
- Walline JJ, Greiner KL, McVey ME, Jones-Jordan LA. Multifocal contact lens myopia control. *Optom Vis Sci* 2013;90:1207–1214.
- Kollbaum PS, Jansen ME, Tan J, Meyer DM, Rickert ME. Vision performance with a contact lens designed to slow myopia progression. *Optom Vis Sci* 2013;90:205–214.
- Sankaridurg P, Holden B, Smith EL, Naduvilath T, Chen X, de la Jara PL, et al. Decrease in rate of myopia progression with a contact lens designed to reduce relative peripheral hyperopia: one-year results. *Invest Ophthalmol Vis Sci* 2011;52:9362–9367.
- Anstice NS, Phillips JR. Effect of dual-focus soft contact lens wear on axial myopia progression in children. *Ophthalmology* 2011;118:1152–1161.
- Atchison DA. Optical models for human myopic eyes. *Vis Res* 2006;46:2236–2250.
- Bakaraju RC, Ehrmann K, Papas E, Ho A. Finite schematic eye models and their accuracy to in-vivo data. *Vis Res* 2008;48:1681–1694.
- Atchison DA, Pritchard N, Schmid KL. Peripheral refraction along the horizontal and vertical visual fields in myopia. *Vis Res* 2006;46:1450–1458.
- Navarro R, Santamaria J. Accommodation-dependent model of the human eye with aspherics. *J Opt Soc Am A* 1985;2:1273–1281.
- Furlan WD, Andres P, Saavedra G, Pons A, Monsoriu JA, Calatayud A, et al. Multifocal ophthalmic lens and method for obtaining same. ES Patent 070559. 2011. WO 2012/028755 A1.
- Saavedra G, Furlan WD, Monsoriu JA. Fractal zone plates. *Opt Lett* 2003;28:971–973.
- Furlan WD, Andres P, Saavedra G, Pons A, Monsoriu JA, Calatayud A, et al. White-light imaging with fractal zone plates. *Opt Lett* 2007;32:2109–2111.
- Furlan WD, Saavedra G, Pons A, et al. Multifocal ophthalmic lens and method for obtaining same. Improvements. ES Patent P201330862. 2012.
- Monsoriu JA, Saavedra G, Furlan WD. Fractal zone plates with variable lacunarity. *Opt Express* 2004;12:4227–4234.
- Phillips J. Contact lens and method US Patent 20080218687 A1. 2008.
- Tabernero J, Schaeffel F. Fast scanning photoretinoscope for measuring peripheral refraction as a function of accommodation. *J Opt Soc Am A Opt Image Sci Vis* 2009;26:2206–2210.
- Calver R, Radhakrishnan H, Osuobeni E, O'Leary D. Peripheral refraction for distance and near vision in emmetropes and myopes. *Ophthalmic Physiol Opt* 2007;27:584–593.
- Davies LN, Mallen EA. Influence of accommodation and refractive status on the peripheral refractive profile. *Br J Ophthalmol* 2009;93:1186–1190.

33. Zemax 13. Optical design program. User's manual. Washington; 2013.
34. Plainis S, Charman WN. On-eye power characteristics of soft contact lenses. *Optom Vis Sci* 1998;75:44–54.
35. Hong XIN, Himebaugh N, Thibos LN. On-eye evaluation of optical performance of rigid and soft contact lenses. *Optom Vis Sci* 2001;78:872–880.
36. Garner L. Front surface topography of spherical flexible contact lenses on the eye. *Aust J Optom* 1977;60:40–45.
37. Cox I. Theoretical calculation of the longitudinal spherical aberration of rigid and soft contact lenses. *Optom Vis Sci* 1990;67:277–282.
38. Legras R, Chateau N, Charman WN. A method for simulation of foveal vision during wear of corrective lenses. *Optom Vis Sci* 2004;81:729–738.
39. Watson AB, Yellott JI. A unified formula for light-adapted pupil size. *J Vis* 2012;12:1–16.
40. Kang P, Swarbrick H. Time course of the effects of orthokeratology on peripheral refraction and corneal topography. *Ophthal Physiol Opt* 2013;33:277–282.
41. Smith EL. Optical treatment strategies to slow myopia progression: effects of the visual extent of the optical treatment zone. *Exp Eye Res* 2013;114:77–78.
42. Sankaridurg P, Donovan L, Varnas S, Ho A, Chen X, Martinez A, et al. Spectacle lenses designed to reduce progression of myopia: 12-month results. *Optom Vis Sci* 2010;87:631–641.
43. Charman WN, Radhakrishnan H. Peripheral refraction and the development of refractive error: a review. *Ophthalmic Physiol Opt* 2010;30:321–338.
44. Faria-Ribeiro M, Queirós A, Lopes-Ferreira D, Jorge J, González-Méijome JM. Peripheral refraction and retinal contour in stable and progressive myopia. *Optom Vis Sci* 2013;90:9–15.
45. Chung K, Mohidin N, O'Leary DJ. Undercorrection of myopia enhances rather than inhibits myopia progression. *Vis Res* 2002;42:2555–2559.
46. Berntsen DA, Kramer CE. Peripheral defocus with spherical and multifocal soft contact lenses. *Optom Vis Sci* 2013;90:1215–1224.
47. Lundström L, Mira-Agudelo A, Artal P. Peripheral optical errors and their change with accommodation differ between emmetropic and myopic eyes. *J Vis* 2009;9:1–11.
48. Whatham A, Zimmermann F, Lazon P, Jara D. Influence of accommodation on off-axis refractive errors in myopic eyes. *J Vis* 2009;9:1–13.
49. Navarro R, Palos F, González L. Adaptive model of the gradient index of the human lens. I. Formulation and model of aging ex vivo lenses. *J Opt Soc Am A* 2007;24:2175–2185.
50. Wang J, Jiao S, Ruggeri M, Shousha MA, Shousha MA, Chen Q. In situ visualization of tears on contact lens using ultra high resolution optical coherence tomography. *Eye Contact Lens* 2009;35:44–49.
51. Hong XIN, Himebaugh N, Thibos LN. On-eye evaluation of optical performance of rigid and soft contact lenses. *Optom Vis Sci* 2001;78:872–880.
52. Maldonado-Codina C, Efron N. Impact of manufacturing technology and material composition on the clinical performance of hydrogel lenses. *Optom Vis Sci* 2004;81:442–454.
53. Tranoudis I, Efron N. Parameter stability of soft contact lenses made from different materials. *Cont Lens Anterior Eye* 2004;27:115–131.
54. Rae SM, Price HC. The effect of soft contact lens wear and time from blink on wavefront aberration measurement variation. *Clin Exp Optom* 2009;92:274–282.
55. Efron S, Efron N, Morgan PB. Repeatability and reliability of ocular aberration measurements in contact lens wear. *Cont Lens Anterior Eye* 2008;31:81–88.